

REVIEW

Interactions between water and organic molecules or inorganic salts on surfaces

Chi Zhang | Wei Xu 

Interdisciplinary Materials Research Center,
College of Materials Science and Engineering,
Tongji University, Shanghai, People's Republic of
China

Correspondence

Wei Xu, Interdisciplinary Materials Research Cen-
ter, College of Materials Science and Engineering,
Tongji University, Shanghai 201804, People's
Republic of China.
Email: xuwei@tongji.edu.cn

Funding information

National Natural Science Foundation of China,
Grant/Award Numbers: 22125203, 21790351;
Fundamental Research Funds for the Central
Universities, Grant/Award Number: 22120210365

Abstract

Water, as a ubiquitous and relatively inert medium, plays a vital role in nature. The interactions between water and organic molecules or inorganic salts are of fundamental interest in understanding hydration processes in chemistry. The combination of scanning probe microscopy and theoretical calculations provides a versatile tool to directly visualize and further rationalize such interactions as well as influences of water on organic molecules and inorganic salts. In this review, we provide a brief overview of the recent exciting progress in revealing the interactions between water and organic molecules as well as inorganic salts (including ions) on surfaces. Herein, we describe first steps of hydration of organic molecules followed by a microsolvation process on surfaces. Subsequently, water-induced tautomerization and chiral separation of small biomolecules on surfaces are discussed for understanding the roles of water in driving biological self-assembly processes. Moreover, water is also able to assist structural transformation globally by selectively interrupting the relatively weak hydrogen bonds within nanostructures. Based on the water-incorporated molecular nanostructures, dissolution of sodium halides on wet surfaces is achievable using confined water, while hydrates of halide ions desorb from the surface. More interestingly, ion hydrates are also demonstrated to be artificially accessible, which enables atomic-scale investigation into local ion hydration and transport at interfaces. This review provides new insights into the role of water in the hydration-related molecular and ionic systems, with implications for hydration and solvent effects down to the single-molecule level.

KEYWORDS

density functional theory, hydration, hydrogen bonds, scanning probe microscopy, water

1 | INTRODUCTION

Water, which covers more than 70% of the surface of the earth, is one of the most ubiquitous chemical substances. Water participates in maintaining the activities of living organisms and is thus essential for life. It has been demonstrated that DNA is heavily hydrated with the formation of hydration shells surrounding,^[1] where water is the medium to dissolve the solute as well as to stabilize the structures. Moreover, it has also been found that water (hydration) may account for the tautomerization of DNA bases, resulting in the presence of rare tautomers and further mispairing and point mutation.^[2–4] Water molecules can provide potential binding sites, which are competitive to those within self-assembled nanostructures of bases, and consequently, hydrogen bonds involved in such nanostructures are greatly suppressed in the water atmosphere.^[1] Besides, water is also

widely applied as a solvent and reactant in chemistry. It is not only indispensably participating in numerous physico-chemical phenomena, such as dissolution, wetting, and corrosion, which can be easily encountered in daily life, but also actively involved in lots of scientific and technological fields such as heterogenous catalysis, corrosion science, and electrochemistry.^[5] As the most abundant and typical solvent, water forms specific intermolecular interactions with solute (subordinate to solute–solvent interactions), along with the breakdown of interactions within solute and the formation of hydration shells around solute. Such hydration shells further enable uniform dispersion of solute-related particles in water. Therefore, it is significant to understand the interactions between water and solute from the standpoint of multiple domains including but not limited to biology, physics, and chemistry. More generally, exploration of the role of water in interacting with organic molecules as well as inorganic salts

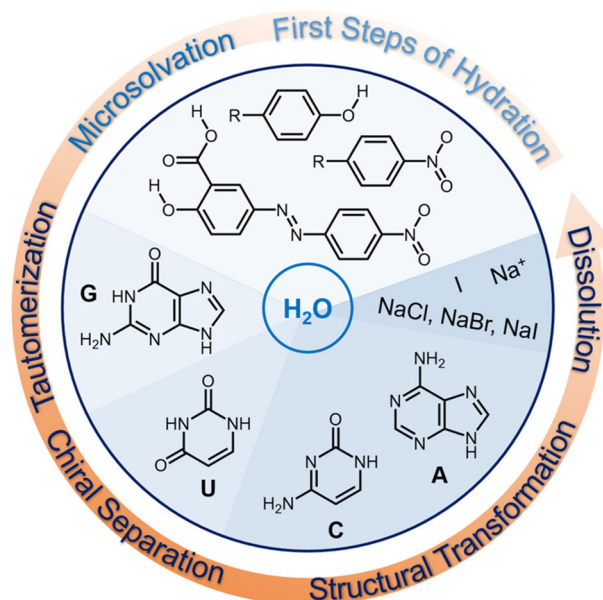
This is an open access article under the terms of the [Creative Commons Attribution](https://creativecommons.org/licenses/by/4.0/) License, which permits use, distribution and reproduction in any medium, provided the original work is properly cited.

© 2022 The Authors. *Aggregate* published by SCUT, AIEI, and John Wiley & Sons Australia, Ltd.

(ions) will provide fundamental insights into molecule and ion hydration, which are closely related to various scientific and technological fields.

The initial step toward understanding the interactions between water and organic molecules as well as inorganic salts (ions) is to construct a well-defined model system. Tremendous efforts have been devoted to the interpretation of such interactions from experiments with techniques such as X-ray crystallography, neutron diffraction crystallography, dielectric relaxation, nuclear magnetic resonance spectroscopy, and various vibrational spectroscopies,^[6–10] while poor spatial resolution and lack of intuitive traits have been the main obstacles. On the other hand, recent decades have witnessed rapid development and progress in surface-science approaches, for instance, scanning tunneling microscopy (STM) and noncontact atomic force microscopy (nc-AFM) combined with X-ray photoelectron spectroscopy (XPS), which give access to real-space structural determination and property detection down to the submolecular or even atomic level.^[11–17] With the substantial contribution of theoretical calculations, these experimental observations can be sophisticatedly interpreted, and the underlying mechanisms are further unraveled. Meanwhile, the two-dimensional (2D) confinement provided by well-defined atomically flat and clean substrates can lead to a simplified template to explore the complicated interactions and dynamics between water and solute in 2D and quasi-2D. Additionally, ultra-high vacuum conditions, under which these surface-science approaches are maintained, are also beneficial for excluding the interference of other chemical substances and controllably regulating the amount of water or solute in the molecular systems. Hence, by means of surface-science approaches, the interactions between water and organic molecules or inorganic salts (ions) can be modeled and studied on surfaces or at interfaces, which enables precise visualization of corresponding structures and dynamics as well as determination of the role of water involved at the submolecular scale.

In this review, we summarize and discuss the recent exciting progress in understanding the interactions between water and organic molecules as well as inorganic salts (including ions) on surfaces (see Scheme 1). As a starting point, before dealing with organic molecules and inorganic salts (ions), we briefly discuss structures and dynamics of pure water molecules on metal oxides, metal substrates, and insulating layers supported by metal substrates. Then, we describe first steps of hydration where water molecules start to attach to isolated organic molecules at low temperatures. As the next step of hydration, a microsolvation process with the formation of solvation shells around specific functional groups of organic molecules is shown on surfaces. Subsequently, we further discuss situations with a much higher water dosage at a substrate temperature of mostly room temperature (RT). We mainly show water-induced tautomerization and chiral separation of small biomolecules for understanding the activities of water in driving biological self-assembly processes. Furthermore, we introduce several studies on water-assisted structural transformation by selectively interrupting the relatively weak hydrogen bonds within molecular nanostructures. Based on the water-incorporated molecular nanostructures, dissolution of sodium halides on wet surfaces by confined water is also shown. Last but not least, based on the sophisticated construction of ion hydrates by tip manipu-



SCHEME 1 Schematic illustration showing several typical examples concerning the interactions between water and organic molecules as well as inorganic salts (ions) on surfaces as detailed in this review. The organic molecules involve 4,4'-hydroxy-azobenzene, 4-anilino-4'-nitro azobenzene, 5-(4-nitrophenylazo) salicylic acid (NPAS), and four bases, that is, guanine (G), uracil (U), cytosine (C), and adenine (A). The inorganic salts include NaCl, NaBr, and NaI. The ions involve I ion and Na⁺

lation, atomic-scale investigation on local ion hydration and transport at interfaces is referred. This review provides new insights into the role of water in molecule and ion hydration in real space, with fundamental implications for hydration and solvent effects from the perspective of a single molecule or ion.

2 | FIRST STEPS OF HYDRATION AND MICROSOLVATION

Due to the vital role of water in nature, the intrinsic physical and chemical properties and phenomena of water molecules have aroused great interests in the field of surface science,^[5,18] with the aim of deep interpretation at the molecular or even submolecular level. Structures and dynamics of water molecules on metal oxides, metal substrates, and insulating layers supported by metal substrates have been extensively investigated. Specifically, the structural formation of water molecules on solid surfaces can shed light on the chemistry of interfacial water. It is known that such a structural formation is mainly governed by the balance between water–water intermolecular interactions (i.e., hydrogen bonds) and water–surface interactions.^[19–20] The nucleation process of water (ice) and the resulting structures on surfaces are closely related to the wetting properties,^[20] which are significant for corrosion and heterogeneous catalysis procedures.

As early as 2001, Besenbacher et al. reported water dissociation on a rutile TiO₂(110) surface,^[21] where oxygen vacancies serve as active surface sites and assist the dissociation process of water molecules through proton transfer. Later, water was found to mediate proton hopping on another metal oxide, FeO(111) monolayer film, and a different proton-transfer mechanism via an H₃O⁺-like

transition state was theoretically revealed.^[22] Besides, the interaction between water and the metastable anatase form of TiO_2 , $\text{TiO}_2(101)$, was explored by He et al., and atomic-scale insights into the hopping of water monomers and ordered water overlayer were provided.^[23] These studies show prototype systems of water molecules adsorbed on metal dioxides, where the substrates are quite complicated due to the local stoichiometry and the surface oxygen atoms involved, which provide additional hydrogen-bonding possibilities.

While, on metal substrates, water–water intermolecular hydrogen bonding usually leads to various water clusters or networks. In 2002, Salmeron et al. reported the dynamics of isolated water molecules on Pd(111) including diffusion and clustering at 40 K,^[20] where water monomers collided with each other to form a pentamer in a stepwise manner, and a hexagonal honeycomb structure was observed upon further water exposure. Such a 2D water overlayer growth on Pd(111) at 100 K was further rationalized by the composition of hexamer rings with a new 2D-water rule,^[24] while the 2D network structures of the first layers of ice on Pt(111) and Ru(0001) at 140 K were found to be composed of various membered rings.^[25–26] Based on these detailed investigations, the scenario about how water monomers diffuse and aggregate to form clusters and further grow into networks in the first wetting layer and multilayers is clearly presented on the single crystals of typical platinum group metals. In addition, substantial attention has also been paid to some other metal substrates such as Cu, Ag, and Au. Michaelides et al. reported the observation and identification of various water nanoclusters on Cu(111) and Ag(111) at low temperatures (i.e., below 25 K),^[19,27] while 1D ice chains constructed by water pentagons were found during the initial stages of ice nucleation on Cu(110) at ~ 100 K,^[28] showing the initial stages of heterogeneous ice nucleation and the growth of water nanostructures on metal substrates. Interestingly, by injecting electrons, Morgenstern et al. successfully controlled the internal hydrogen bonds involved in the water nanoclusters adsorbed on Ag(111).^[29] Moreover, Okuyama et al. also observed 1D anisotropic water chain growth on Cu(110) at 78 K^[30] and further investigated the dynamics within water dimers on Cu(110) at 6 K with a hydrogen-bond rearrangement.^[31] Recently, with the aid of bond-resolved nc-AFM imaging, Sugimoto et al. visualized the atomic structures of pentagonal water chains (after deposition at 78 K) as well as hexagonal water-hydroxyl networks caused by partial dissociation (after annealing at 160 K) on Cu(110) based on the oxygen skeletons involved, where local defects and edges were also unambiguously revealed.^[32] Additionally, a detailed water nucleation process was explored on a more inert Au(111) surface as well by Hrbek et al., in which the substrate was found to be hydrophobic and the weak water–surface interaction resulted in the formation of a unique double bilayer.^[33] For deeper understanding of the submolecular water structures, Jiang et al. clearly resolved the internal structure of individual water monomers and tetramers on an insulating NaCl(001) film supported by Au(111),^[34] visualized proton tunneling in the water tetramer,^[35] and also probed the growth of water nanoclusters and formation of 2D bilayer ice structure.^[36] Based on the comprehensive investigations concerning water molecules adsorbed on various substrates as discussed above, we now have a brief overview of the growth of water nanostructures in terms of

decreasing water–surface interactions, indicating the wetting processes at the nanometer scale. Much more details have been systematically covered by the excellent review papers by Michaelides et al.^[5] and Salmeron et al.^[18] and are thus skipped herein.

With tremendous attention paid to water itself, one interesting question is how water interacts with organic molecules during the initial hydration processes. To explore the starting and following steps of water molecules interacting with organic molecules, Morgenstern et al. first applied 4,4'-hydroxy-azobenzene and 4-anilino-4'-nitro azobenzene molecules adsorbed on an inert metal surface, Au(111), to construct the model system.^[37] The two organic molecules are mainly functionalized with hydroxyl and anilino groups, respectively, and the first one is typically shown in Figure 1A.

4,4'-hydroxy-azobenzene was deposited onto Au(111), and each molecule appeared in a dumbbell shape (Figure 1A). The hydroxyl groups located at both ends of the molecule may have different conformations with respect to the molecular axis, and different relative orientations may also exist in the azobenzene part, resulting in the series of possibilities involved. Due to the absence of submolecular details, it was difficult or even impossible to discriminate the molecular conformation of a single molecule. After coadsorption of small amounts of water molecules, the first solvation shells appeared at the vicinity of hydroxyl groups due to the formation of hydrogen bonds (cf. Figure 1B and C). Interestingly, given that hydrogen bonds are directional, the position of a single water molecule with respect to the molecular axis can be applied as a criterion to determine the molecular conformation of 4,4'-hydroxy-azobenzene. Based on the relative angles and positions, the authors successfully achieved the determination of molecular conformation, as shown in the superimposed structural models in Figure 1B and C. It is also worth noting that initially, water molecules attach to the hydroxyl groups exclusively, and additional water molecules tend to form hydrogen-bonded clusters as shown in Figure 1D–L. Similarly, the additional ones were also used to identify the orientation of water molecules in the first step. With an increasing ratio of water in the molecular system, more water accumulates at the ends, and gradually, water clusters with 3D structures cannot be resolved molecularly (Figure 1L). Furthermore, 4-anilino-4'-nitro azobenzene was also codeposited onto Au(111) with water to corroborate the generality of the structural determination based on the hydration shells. Both cases nicely demonstrated that water attaches to the polar functional groups (hydroxyl and nitro groups) in the first steps of hydration, which seeds the formation of hydration shells.

For the detailed exploration of microsolvation of an organic molecule, 5-(4-nitrophenylazo) salicylic acid (shortened as NPAS thereafter), which is functionalized with groups of different water affinity (carboxyl, hydroxyl, and nitro groups), was investigated by Morgenstern et al. on Au(111).^[38] After coadsorption of NPAS and D_2O , water molecules preferentially attached to the carboxyl and nitro groups (cf. Figure 1M and N), which account for 53% and 37% in the first step of hydration, respectively. Accordingly, carboxyl group shows a higher water affinity compared to nitro group, and both of them are much more hydrophilic than the diazo group and phenyl rings. Interestingly, it was experimentally verified that water would not bind to the hydroxyl

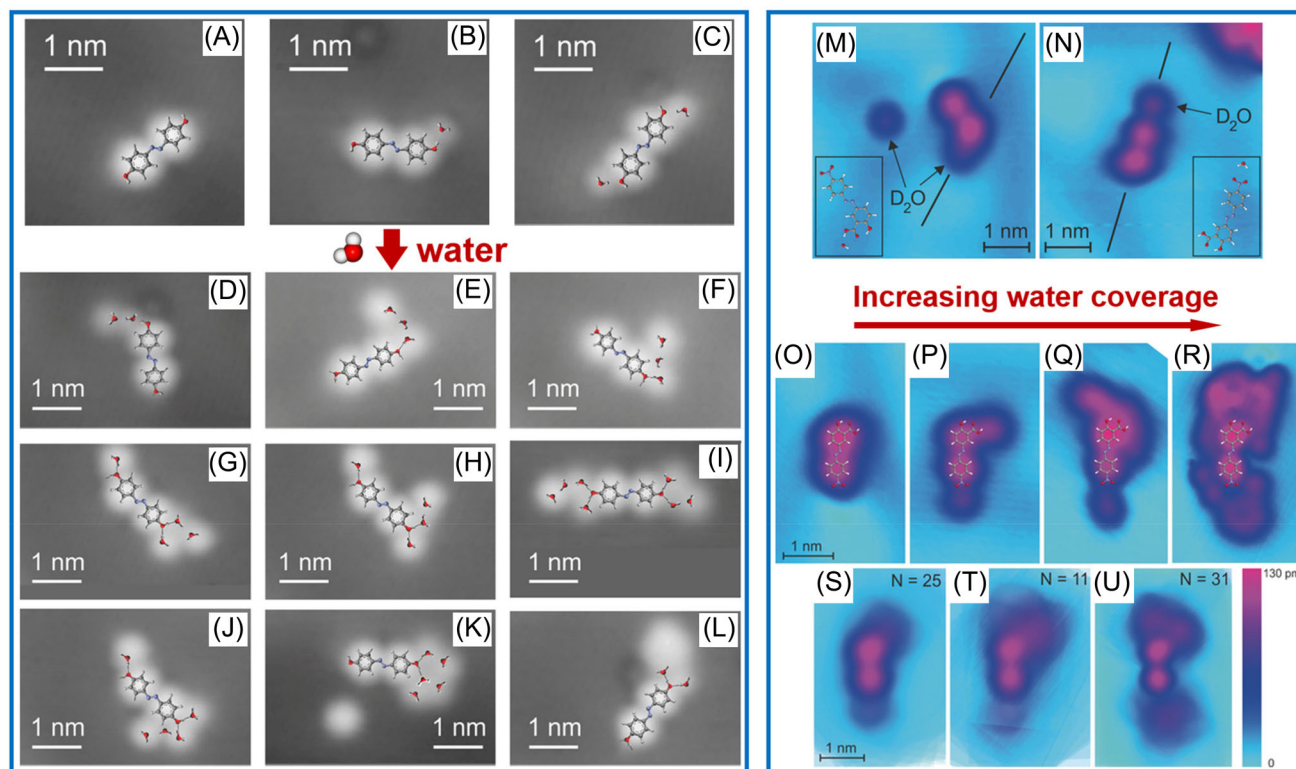


FIGURE 1 First steps of hydration based on 4,4'-hydroxy-azobenzene^[37] (left panel) and microsolvation processes based on NPAS molecule^[38] (right panel). (A)–(C) STM images showing (A) a single 4,4'-hydroxy-azobenzene molecule on Au(111), and (B)–(C) with water molecules attached at one or two ends. (D)–(L) STM images showing further hydration of 4,4'-hydroxy-azobenzene. The corresponding structural models are superimposed on the STM images, respectively. (M)–(N) Single water molecules attached to NPAS on Au(111). (O)–(R) Hydration of the NPAS molecule starting from (O) a pristine molecule, in response to (P)–(R) an increasing water coverage. (S)–(U) Stacked STM images (with the number denoted as N) corresponding to the three preparations in (P)–(R). C: gray; H: white; N: blue; O: red. (A)–(L) Reproduced with permission from Ref. 37: Copyright 2014, American Chemical Society. (M)–(U) Reproduced with permission from Ref. 38: Copyright 2018, John Wiley and Sons

group before the occupation of carboxyl group. Therefore, from the formation of solvation shell, the hydrophilicity of the functional groups can be traced, which is in the order of carboxyl group > nitro group > hydroxyl group > diazo group or phenyl rings. After further increasing the water coverage step by step, 2D solvation shells were obtained as shown in Figure 1O–U. Obviously, water was attracted by the carboxyl and nitro groups exclusively in the beginning (Figure 1P), followed by the formation of solvation shells around the attached water molecules (Figure 1Q). Note that when the solvation shells grew larger, the influence of functional groups decreased, and the entire molecule was surrounded by water molecules (Figure 1R). To show the lateral probability distribution of water according to the specific ratio shown in Figure 1P–R, sets of STM images were stacked together (cf. Figure 1S–U). The carboxyl and nitro groups served as nucleation centers, while more water accumulated around the carboxyl group, in agreement with the preference discussed above in the first steps of hydration (Figure 1S). At a gradually increasing water ratio, the solvation shells further extended, and surprisingly, diazo group and phenyl rings were hydrophobic with no water attached consistently (Figure 1T). The full solvation of NPAS molecule was achieved at an even higher water ratio (Figure 1U). Consequently, by incorporating different functional groups into the same organic molecule, the respective hydrophilicity was experimentally demonstrated in real space with a submolecular resolution. Meanwhile, the stepwise formation of solvation shells around the organic molecule was also clearly displayed, with fasci-

nating insights into the microsolvation process at a single-molecule level.

In view of the hydration process, polymorphic arrangement of the water-NPAS complexes on Au(111) was further explored by the same group,^[39] showing the interactions between hydrated motifs. Besides, the influence of water on the self-assembled structures of 4,4'-dihydroxy azobenzene was detected on Ag(111),^[40] where water directly interacted with hydroxyl end groups with changes in the supramolecular structures. As an extension, the 1D hydrogen-bonded solid chains made up of 3-methoxy-9-diazafluorene (MDAF) on Ag(111) were exposed to solvation environment, which resulted in the water-decorated MDAF chains at 25 K and water-MDAF nanoclusters (with a D₂O cluster as the core) upon annealing to 80 K.^[41] Such a phenomenon thus indicates the relative strength of interactions involved in the dissolution of MDAF chain structures, that is, D₂O-D₂O > D₂O-MDAF > MDAF-MDAF.

Besides, recently, the interaction between water and organic molecules at low temperatures also aroused the attention of Hodgson et al., and the hydration of a 2D bitartrate supramolecular nanostructure on Cu(110) was investigated responding to increasing surface temperatures in the range of 80–150 K.^[42] During such a process, water changed the adsorption sites as driven by the creation of stable ones, implying the temperature-dependent evolution of hydration layers on a metal surface.

It is noteworthy that in the vast majority of above-mentioned situations, water pressure is in the range of

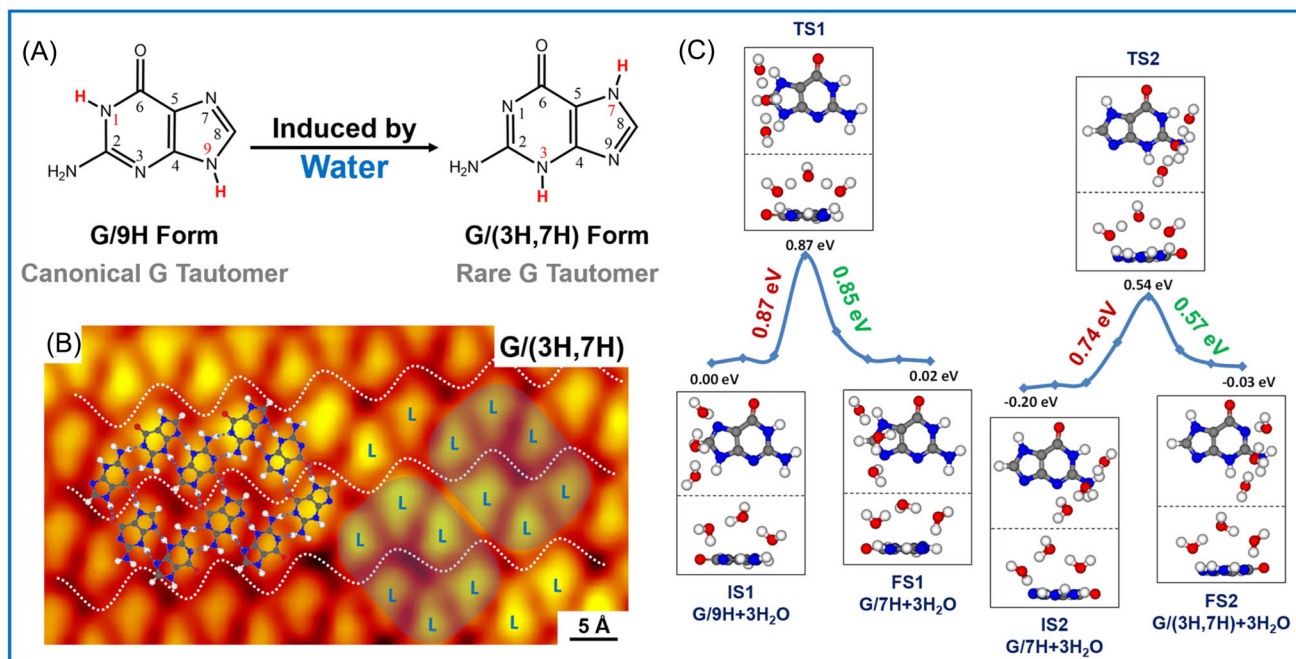


FIGURE 2 Water-assisted tautomerization of guanine from G/9H to G/(3H,7H) on Au(111).^[48] (A) Schematic illustration of the tautomerization from G/9H to G/(3H,7H). (B) STM image showing the formation of network structures composed of parallel six-membered rings with the same molecular chirality, which is characteristic for G/(3H,7H) tautomer. The DFT optimized structural model of the network is superimposed and hydrogen bonds are depicted by dotted lines. (C) DFT calculated reaction pathway for the tautomerization with the assistance of water bridges. Reproduced with permission from Ref. 48: Copyright 2016, American Chemical Society

10^{-7} mbar or even below, with the coadsorption of organic molecules on metal substrates held at relatively low temperatures ca. <30 K. These studies thus provide fundamental insights into the first steps of hydration and microsolvation of single molecules at low temperatures.

3 | TAUTOMERIZATION

Apart from the role as a solvent, water is also significant in the metabolic processes. It may be responsible for the tautomerization of bases, resulting in the presence of rare tautomers and further mispairing and point mutation.^[2–4] Numerous theoretical studies have been carried out in order to explore the intramolecular proton transfer processes in the possible tautomeric forms of DNA bases.^[2–4,43–47] For instance, Hobza et al. systematically investigated several DNA bases and their tautomers under different conditions, including gas phase, a microhydrated environment (with one and two water molecules), and aqueous solution.^[2,43–45] Accordingly, they found that bulk water is able to greatly change the relative stability of tautomers and even affect the global minimum involved. Interestingly, the relative stability order of guanine (G) tautomers is unchanged in a microhydrated environment, while three rare tautomers are highly favored with the involvement of bulk water, leading to the variation in the tautomeric equilibrium.^[2] Moreover, it was also predicted that water can assist tautomerization processes by providing a lower energy barrier.^[47]

Despite the valuable insights from a theoretical perspective, real-space evidence of the water-assisted tautomerization has been less reported. As motivated by this, Xu et al. explored the tautomerization of G molecules on Au(111) under water atmosphere^[48] (cf. Figure 2). G has various tau-

tomeric forms including the canonical G/9H and noncanonical G/7H forms as the two most stable ones.^[49] The tautomerization process from G/9H to G/7H on Au(111) can be induced by thermal treatment with an obvious change in the self-assembled structures, which was successfully inhibited by the involvement of Ni atoms in occupying the N7 site of G/9H.^[49] Moreover, as G-quartet-M (M: Na/K/Ca) complexes were successfully obtained by applying alkali and alkaline earth salts to interact with 9-ethylguanine,^[50] the G/9H and G/7H tautomers involved in a mixture phase on Au(111) could be further recognized and separated with the assistance of NaCl.^[51] Interestingly, the corresponding tautomeric pure phases were thereafter fabricated by annealing (forming a pure G/7H phase) and interacting with NaCl (generating a G-quartet-Na structure composed of G/9H), respectively,^[51] indicating the interconversions between tautomers.

On the foundation of previous research findings, the water-induced tautomerization from G/9H to a rare G/(3H,7H) tautomer was explored (Figure 2A). By exposing the disordered mixture phase mainly made up of G/9H and G/7H to the water atmosphere at a pressure of $\sim 10^{-5}$ mbar at RT, six-membered ring structures connected by chains were observed at a low molecular coverage. Direct deposition of G molecules under the same water condition along with regulation on the molecular coverages led to big patches of six-membered ring structures coexisting with chains. Interestingly, lower water pressures were not capable of inducing the structural transformation, indicating a certain role of bulk water herein. Further gentle annealing the sample to 310 K brought about large network structures composed of six-membered rings as typically shown in Figure 2B, which are in the same chirality and different from the racemic G/7H phase.^[49] Besides, parallel six-membered rings were involved instead of orthogonal ones in

the G/7H phase. Considering the previous theoretical investigations, real-space evidence, as well as DFT calculated structures, only the rare tautomeric G/(3H,7H) form can rationalize the ring structures with reasonable intermolecular hydrogen bonds. Therefore, other tautomers were ruled out, and the tautomerization to G/(3H,7H) was experimentally evidenced. To further demonstrate the water-induced tautomerization and unravel the underlying mechanisms, DFT calculations were performed to reveal the reaction pathways involved in the tautomerization processes without and with the participation of water molecules. In the absence of water molecules, the tautomerization from G/9H to G/(3H,7H) involves proton transfer from N1 to N3 generating G/(3H,9H) as an intermediate and from N9 to N7 forming the final product G/(3H,7H). During such a process, the reaction barrier was determined to be 1.91 eV, which is too high for the process to take place without any external stimuli under anhydrous conditions. Taking into account the bulk water instead of microhydrated environment in the experiment, the authors involved three water molecules to construct the structural models in DFT calculations for each proton-transfer process either from N9 to N7 or from N1 to N3 (Figure 2C). Three water molecules connect either the imidazole ring or the pyrimidine ring by forming series of hydrogen bonds, and they are suspended over the G molecular plane as a water bridge. Interestingly, the proton transfer could easily take place one by one like the domino effect from one side to the opposite side with the assistance of water bridges. The two hydrogen-bonded proton-transfer loops thus significantly reduced the reaction barriers for the corresponding tautomerizations, which were calculated to be 0.87 and 0.74 eV, respectively (see Figure 2C). Although more water molecules should be involved under the experimental conditions, such a process unambiguously indicates the significant role of water in facilitating the tautomerization processes and formation of rare tautomers. Moreover, water-mediated hydrogen bonds highly promoted the proton transfer, while water was not finally found on Au(111), acting as a good leaving molecule.

4 | CHIRAL SEPARATION

Water plays a crucial role in driving biological self-assembly processes, and it may also be related to the chirality issues in biologically related systems. Moreover, it has been demonstrated that water is involved in processes of chiral generation, amplification and inversion *in vitro*. With high motivation of real-space understanding about how water engages in biomolecular chirality related issues, Xu et al. explored the influence of bulk water on the uracil (U) self-assembled structures on Au(111)^[52] (cf. Figure 3).

Upon deposition of U onto Au(111), a close-packed U structure was obtained (Figure 3A), which was identified as a racemic phase with a mixture of two chiralities from nc-AFM images. Structural transformation to an ordered racemic phase can be achieved by annealing to 330 K. By exposing either the disordered or ordered racemic U structures to water atmosphere of $\sim 8 \times 10^{-5}$ mbar at RT, an obvious phase transition to porous network structures was observed (Figure 3B). Such porous structures were in different organizational chiralities as resolved from the cavities involved. From the magnified STM images (Figure 3C–E and H), it can be confirmed

that water molecules are confined in the porous structures, which appear as round protrusions (highlighted by white circles) at the centers of U pentamers (depicted by pentagon contours). The chirality of each U molecule involved was further clearly recognized from the molecular skeletons offered by the corresponding nc-AFM images of the two networks (Figure 3F and I), indicating that homochiral U molecules interact with water molecules forming porous networks via intermolecular hydrogen bonds. The DFT calculated structural models superimposed on the bond-resolved nc-AFM images (Figure 3G and J) further showed the detailed hydrogen-bonded configurations of pentamers, where N–H...O and O–H...O hydrogen bonds were formed among U molecules and between U and water molecules, respectively. Therefore, the two porous networks were attributed to homochiral U+H₂O structures with opposite U chiralities involved. Accordingly, the water-induced chiral separation was successfully achieved in a global manner, accompanied by the structural transformation from close-packed racemic phases (either disordered or ordered) to porous homochiral U+H₂O structures. Furthermore, holding the sample covered with homochiral U+H₂O structures at RT for 1.5 h resulted in the water desorption and reversed structural transformation back to an ordered racemic U structure. As for the origin of such a chiral separation, a preferential binding between water and a specific site of U (O1) was determined both experimentally and theoretically, which resulted in the generation of homochiral (U–H₂O–U)₂ cluster and eventually 2D homochiral U+H₂O structures. Note that in this work, the H₂O–U interactions were undoubtedly distinguished from the nc-AFM imaging, leading to the atomic-scale discrimination of hydrogen-bonded configurations in real space. Meanwhile, the application of qPlus-sensor-based nc-AFM with functionalized tips (CO in this case) proves to be indispensable, as it provides the possibility to directly probe the molecular skeletons as well as intermolecular hydrogen bonds with ultrahigh resolution, which is superior to the round topographic information identified from STM images.

Herein, interestingly, the interaction between water and organic molecule U is somehow comparable to that between U molecules, and thus water molecules could be trapped in the molecular structures. The global chiral separation achieved by introducing water molecules merely at RT shows the magic power of water in the biological systems at a single-molecule level, which not only serves as a solvent medium, but also drives the molecular self-assembly processes by providing additional hydrogen-bonding interactions. Nevertheless, the exact role of water in the origin of chirality *in vivo* may be still far beyond our current understandings and will be left as an open question in the fields of biology and chemistry.

5 | STRUCTURAL TRANSFORMATION

Despite the specific role of water in the chiral separation of U structures, the core driving forces in the combined systems of water and organic molecules mentioned above should be intermolecular hydrogen bonds. Different hydrogen-bonded configurations usually lead to distinct self-assembled structures and patterns, and consequently, structural transformation can be treated as a characteristic feature for the judgment of variation in intermolecular hydrogen bonds. The

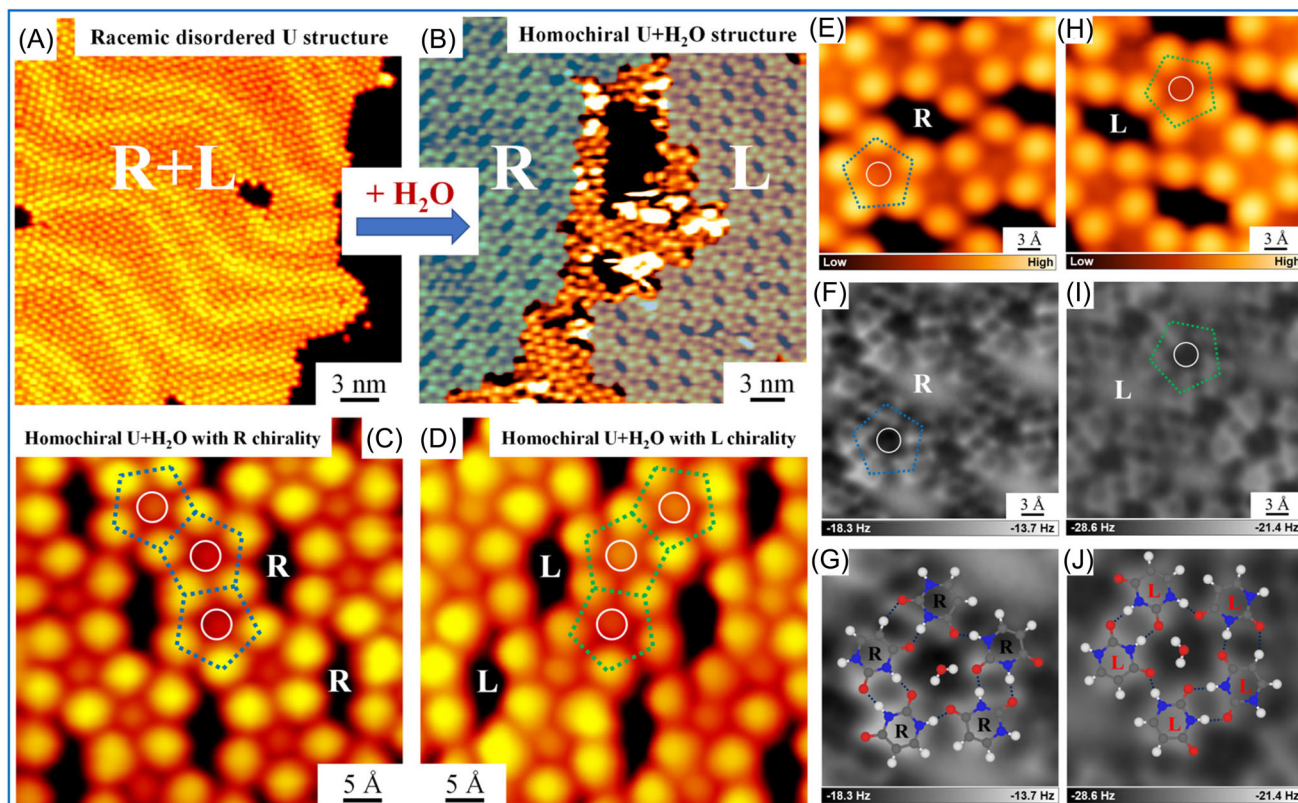


FIGURE 3 Water-induced chiral separation from a racemic U structure to a homochiral U+H₂O structure on Au(111).^[52] (A), (B) Large-scale STM images showing a racemic U self-assembled structure and separated homochiral U+H₂O islands with two opposite chiralities (A) before and (B) after introducing water into the U molecular system. (C), (D) Magnified STM images showing the U+H₂O structures with (C) R and (D) L chiralities. (E), (F), (H), (I) High-resolution STM and nc-AFM images of the two U+H₂O islands. (G), (J) Zoomed-in nc-AFM images of five-membered rings with U in R and L chiralities. The corresponding DFT calculated structural models were superimposed with hydrogen bonds depicted in dotted lines. Reproduced with permission from Ref. 52: Copyright 2021, American Chemical Society

recent studies on water-induced structural transformation presented by Xu et al. clearly show the global interference of water on the preassembled nanostructures made up of organic molecules.^[53–54]

The well-known glassy-state cytosine (C) random networks^[55] on Au(111), which were composed of diverse hydrogen-bonded dimers, were applied to demonstrate the interference and influence of water atmosphere on the C structures^[54] (cf. Figure 4). After exposure to water atmosphere of 1×10^{-5} mbar, surprisingly, 1D quasi-linear C chains appeared in parallel (Figure 4I) instead of T-junction C chains (Figure 4A). The zoomed-in STM image displayed various T-junctions as indicated by red arrows before water exposure (Figure 4B). From the sets of STM and nc-AFM images of two typical T-junctions (Figure 4C–H), the hydrogen-bonded configurations were directly visualized and the corresponding models were further superimposed on the nc-AFM images (Figure 4E and H). Based on the bond-resolved nc-AFM images, previous reports on C tautomers as well as extensive DFT calculations, the authors proposed that strong hydrogen-bonded dimer configurations (i.e., dimer 1–8, with hydrogen bonds depicted in green) and weak ones (i.e., dimer 9–14, with hydrogen bonds depicted in red) were involved in the molecular chain segments and T-junctions, respectively. Upon water exposure, 1D extended C chains were parallel aligned on Au(111) (Figure 4J). High-resolution STM and nc-AFM images (Figure 4K and L) further provided submolecular information involving the hydrogen-bonded configurations, which led to the structural

assignment as shown in Figure 4M. It is noteworthy that the 1D C chain was composed of strong hydrogen-bonded dimer configurations (i.e., dimer 1–8), while weak ones did not participate in the structures.

Further DFT calculations revealed that for the strong dimers, at least one hydrogen bond was stronger than the water-involved hydrogen bonds in the hydrated C structures (i.e., C-H₂O clusters), while all the hydrogen bonds within the weak dimers were calculated to be weaker than those within the corresponding C-H₂O clusters. Therefore, the weak dimers could be disturbed by water molecules by forming water-involved stronger hydrogen-bonded configurations. In contrast, the strong dimers could be preserved after water exposure. Molecular dynamics simulations of the growth processes of C chains with T-junctions and 1D C chains induced by water are shown in the lower panel of Figure 4. The whole process involves (1) C self-assembly process forming T-junction C chains with both strong and weak cytosine-cytosine (shortened as C-C) hydrogen bonds in the beginning, (2) selective breakage of weak C-C hydrogen bonds and substitution with stronger C-H₂O hydrogen bonds, and (3) further construction of even stronger C-C hydrogen bonds with the releasing and desorption of water molecules. Eventually, 1D quasi-linear C chains appeared with different hydrogen-bonded configurations. One interesting point here is that water molecules selectively break weak intermolecular C-C hydrogen bonds, which efficiently leads to the variation in intermolecular hydrogen-bonded configurations (to form more stable ones) featured by a complete structural

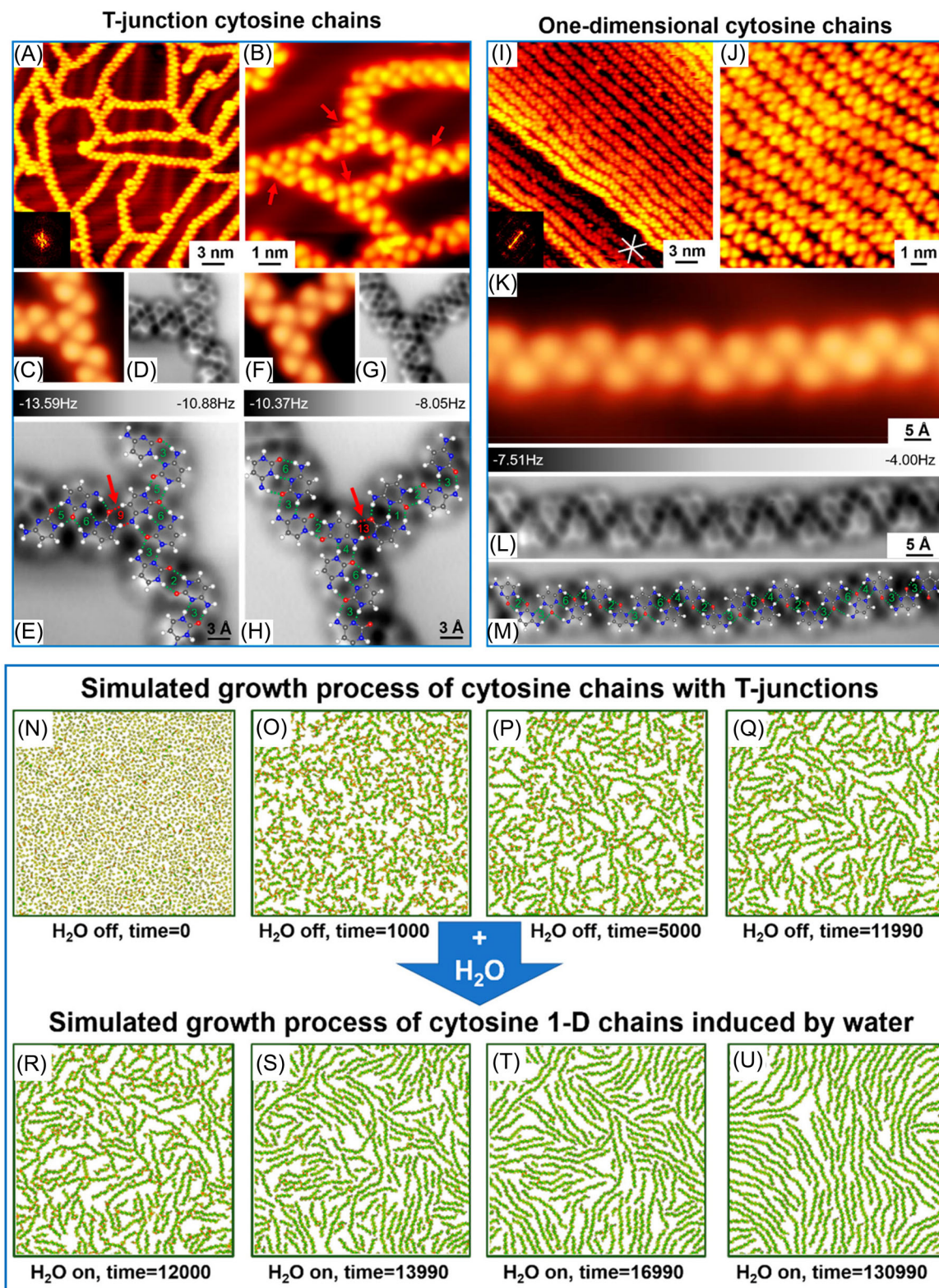


FIGURE 4 Water-induced structural transformation from T-junction C chains to 1D quasi-linear C chains on Au(111).^[54] (A)–(M) STM and nc-AFM images showing (A)–(H) the T-junction C chains before water exposure and (I)–(M) 1D C chains upon water exposure. (A) Large-scale STM topography and (B) zoomed-in STM image showing the randomly distributed T junctions. (C)–(E), (F)–(H) Sets of STM and nc-AFM images and proposed models of two typical T junctions. (I) Large-scale STM topography and (J) zoomed-in STM image showing the 1D extended C chains. (K)–(M) A set of STM and nc-AFM images and a proposed model of a 1D C chain. The strong hydrogen bonds (within stable dimer configurations) were depicted by green dotted lines, while the weak ones (within weak dimers) were depicted by red dotted lines. (N)–(U) Molecular dynamics simulations on the growth processes of (N)–(Q) C chains with T-junctions and (R)–(U) 1D C chains induced by water. Green and red dots indicate strong and weak hydrogen bonds, and water-involved hydrogen bonds are depicted in blue dots. Reproduced with permission from Ref. 54: Copyright 2020, American Chemical Society

transformation. On the contrary, such a process could not be accessed by thermal treatment, which might break both weak and strong ones simultaneously, showing the catalytic role of water in the whole processes.

Another example of structural transformation is the water-induced scission and stitching of adenine (A) self-assembled structures on Au(111) reported by the same group earlier.^[53] In the absence of water, biomolecule A self-assembled into islands composed of characteristic six-membered rings in each row.^[56] When the sample was further exposed to the water atmosphere of $\sim 1 \times 10^{-6}$ mbar at RT, A islands disassembled into molecular rows while water molecule may diffuse along the edges. A higher water pressure of $\sim 1 \times 10^{-5}$ mbar and $\sim 3 \times 10^{-5}$ mbar at RT then resulted in the gradual formation and growth of rectangular islands consisting of A molecular rows and bright dots, which were assigned to A-H₂O islands. Detailed comparisons together with DFT calculations revealed that A molecular rows were well preserved, while the interrow hydrogen-bonded configurations with the lowest stabilization energy were cleaved with the involvement of water molecules. Water molecules further interacted with A molecular rows forming additional hydrogen bonds. Further interconversion between A-H₂O islands and A molecular rows could be obtained by introducing water and removing water via annealing, exhibiting the interference of water on the hydrogen-bonded configurations. Moreover, the gradual structural evolution of preassembled A molecular structures in response to water atmosphere presents an interesting example of dynamic hydration processes of organic molecules at RT.

From the above examples, we have discussed the structural transformations of preassembled 1D and 2D organic nanostructures on surfaces caused by water at RT, where the competition among hydrogen bonds involved in water and organic molecules plays a key role. Notably, subtle differences in the strength of hydrogen bonds may be smartly detected by water molecules, leading to distinct assembled phenomena and patterns, while whether water molecules are finally integrated or not may highly depend on the local hydrogen-bonded configurations and the corresponding stabilities.

6 | DISSOLUTION OF SALTS AND HYDRATION OF IONS

Extended from the intriguing interactions and phenomena between water and organic molecules, the influence of water on the inorganic salts and ions has also been an attractive topic in the field of surface science recently. As an omnipresent phenomenon in nature, salt dissolution is closely linked to the interactions between water and salts as well as the hydration of ions, and it is thus of general interest to directly observe such processes in real space at a submolecular or even atomic level.

By confining water molecules in two dimensions, Xu et al. focused on the dissolution of three sodium halides, that is, NaCl, NaBr, and NaI, on Au(111).^[57] Inspired by the previous finding that A molecules can trap water from gas phase to Au(111) by forming A-H₂O structures with water embedded,^[53] they applied A nanostructures as a reservoir to study the salt dissolution on Au(111). A molecules and NaCl were first codeposited onto Au(111) at RT leading to charac-

teristic A nanostructures and NaCl islands with phase separation (Figure 5A). Further exposure to the water atmosphere of $\sim 10^{-3}$ mbar brought about A-H₂O structures together with NaCl islands (Figure 5B). Interestingly, after releasing water molecules by annealing, 1D straight chains appeared with the vanishing of NaCl islands (Figure 5C). A control experiment by codepositing A and Na onto Au(111) and annealing resulted in the same chain structures and further corroborated the composition of such straight chains (Figure 5D), which was revealed to be A₄Na₂ structure based on DFT calculations (Figure 5E and F). Besides, the coexisting phase of A and NaCl (as shown in Figure 5A) stayed the same after annealing until A desorption, which implied the absence of Cl⁻ under the condition of Figure 5C. Additionally, other salts (NaBr and NaI) displayed similar processes. Therefore, the scenario of desorption of Cl⁻/Br⁻/I⁻ hydrates was concluded, indicating the dissolution process of sodium halides on surface. As an extension, the hydration of halogen (I₂) was investigated alone on Au(111) recently to avoid the interference of metal cations.^[58] The I hydration on Au(111) at a water pressure of $\sim 10^{-3}$ mbar at RT was found to be accompanied by the desorption of hydrates. A combination of XPS spectra and STM imaging shows a gradual decrease in the intensities of I 3d peaks until they totally vanished with the recovery of a clean surface. Furthermore, by applying the self-assembled structure of nickel-phthalocyanine (NiPc) as a template to host I atoms, the number of I atoms can be regulated, and a stepwise hydration of I with an increasing water dosage was clearly visualized. Herein, XPS, as a quantitative technique for measuring the elemental composition of the surface, provides complementary information to the topography obtained by STM imaging.

More interestingly, Jiang et al. systematically constructed several Na⁺ hydrates, that is, Na⁺·nD₂O clusters ($n = 1-5$), on NaCl/Au(111) by tip manipulations, and further experimentally characterized their transport properties.^[59] In the first step, individual water (D₂O) molecules were attached to Na⁺ progressively, forming the corresponding Na⁺·nD₂O clusters in a controlled manner as schematically shown in Figure 5G. The resulting geometries, STM and nc-AFM images, together with AFM simulations clearly showed the real-space atomic-scale visualization of each hydrates. Na⁺ ion appears as a depression in the nc-AFM images, while the brightness of D₂O is related to the adsorption geometry involved (either standing or flat lying). Then, by injecting hot electrons or holes into the substrate, the diffusion probability of Na⁺·3D₂O and Na⁺·3H₂O was experimentally determined in response to bias voltages, and an abrupt jump starting from ± 150 mV (± 170 mV) was attributed to the bending mode of D₂O (H₂O). Furthermore, Na⁺·3D₂O was found to be the most mobile one under a Cl⁻ tip by vibrational excitation. Extensive DFT calculations revealed that it has a diffusion barrier of <80 meV, which was the lowest among the five hydrates owing to the existence of a metastable state. These striking findings thus shed light on local ion hydration and transport at interfaces down to the atomic level. For comprehensive overviews of the sophisticated high-resolution AFM techniques in probing water–solid interfaces, interested readers are also referred to the nice review^[60] by Jiang et al. recently.

Simultaneously, the dissolution of NaCl islands on Au(111) below the freezing point also attracted the attention

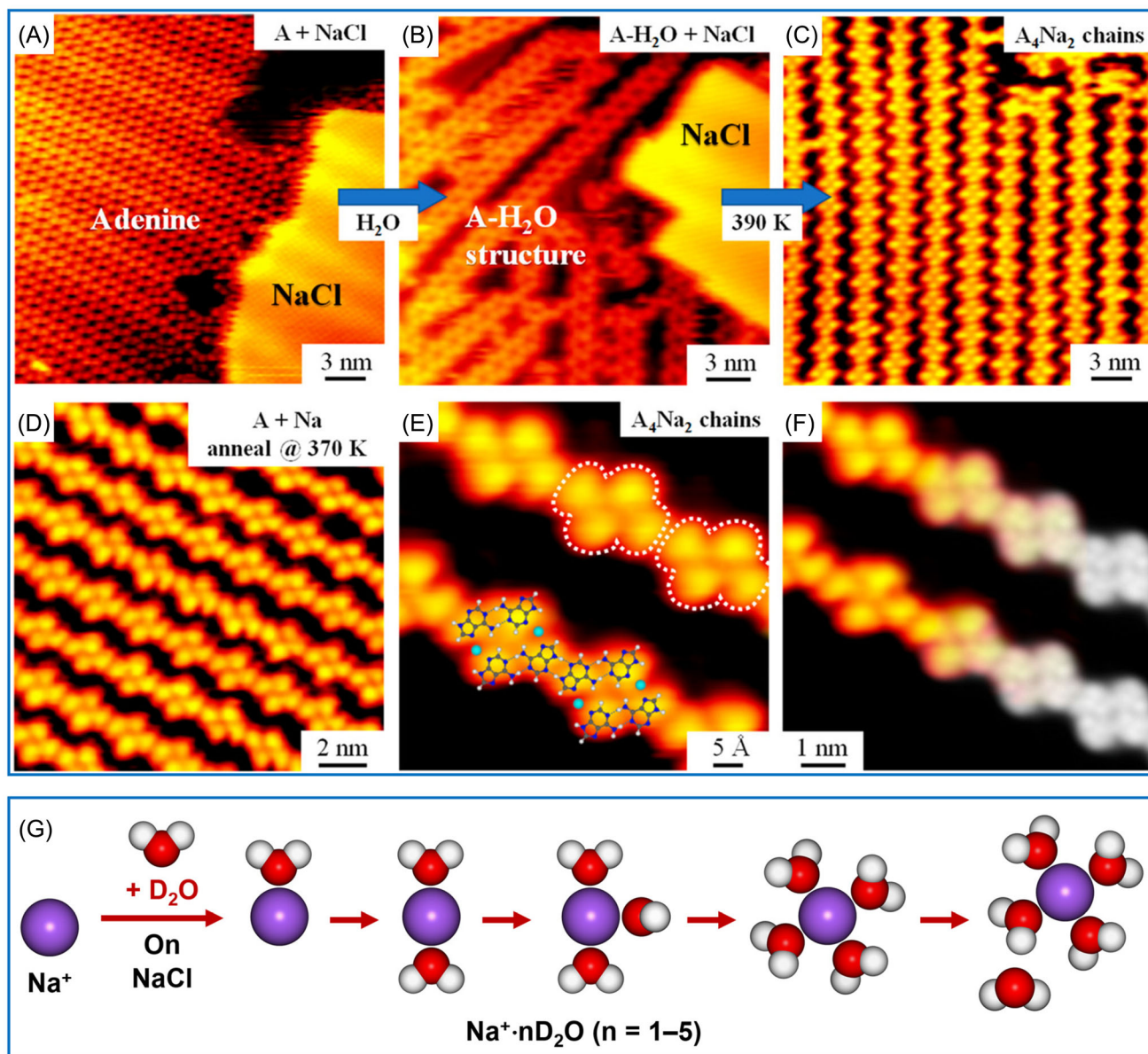


FIGURE 5 Water-induced dissolution of NaCl on Au(111)^[57] (top panel) and hydration of Na⁺ on NaCl/Au(111)^[54] (bottom panel). (A)–(C) A set of STM images showing (A) phase separation after codeposition of A molecules and NaCl onto Au(111) at RT, (B) formation of A-H₂O structures coexisting with NaCl islands after water exposure at RT, and (C) evolution to A₄Na₂ chains after annealing at 390 K with the desorption of Cl⁻ and water. (D)–(F) Large-scale and zoomed-in STM images showing the formation of A₄Na₂ chains after codeposition of A and Na on Au(111) and annealing at 370 K. DFT optimized structural model and STM simulation (in gray) are superimposed on E and F, respectively. (G) Schematic illustration showing Na⁺·nD₂O clusters ($n = 1-5$) constructed on NaCl/Au(111).^[59] (A)–(F) Reproduced with permission from Ref. 57: Copyright 2019, American Chemical Society

from Jiang et al.,^[61] and NaCl bilayer covered with a 2D ice overlayer was taken as a model system. It was found that NaCl dissolution started from the step edges at 145 K, and its decomposition and restructuring took place at 155 K with the desorption of water, which provides an important clue to the initial stage of NaCl dissolution at low temperatures globally.

7 | SUMMARY AND PERSPECTIVE

In summary, in this review, we have mainly summarized several typical studies on the interactions between water and organic molecules as well as inorganic salts (ions) on surfaces, with the aim of better understanding of the chemical and physical properties of water at interfaces. Tremendous striking progress has been achieved in new understanding and knowledge in the following aspects: (1) the first

steps of hydration and microsolvation, including hydrophilicity and hydrophobicity of different functional groups at the single-molecule level; (2) the role of water in biologically related issues, such as tautomerization of bases and chirality of biomolecules; (3) the cooperation and competition between intermolecular interactions among water and organic molecules as well as inorganic salts (ions) in a global manner; and (4) the detailed structures and dynamics of hydrated molecules and ions at interfaces at the atomic scale. Nevertheless, there remain many open questions to be solved in the near future in terms of developing experimental techniques and theoretical models and further establishing methodologies in precise visualization and interpretation of detailed hydration processes for modeling the dynamics. In this sense, combination of various atomic-scale topographic characterization techniques (such as bond-resolved STM^[14,62] and nc-AFM^[63–64]) and precise spectroscopic

techniques with single-chemical-bond sensitivity (such as tip-enhanced Raman spectroscopy^[65–66]) would give valuable and complementary indications involving both skeleton and chemical information in water-incorporated dynamic processes. Moreover, most of studies discussed here have been devoted to the well-defined solid surfaces under ultrahigh vacuum conditions as simplified model systems, while significant differences exist between the model systems and the ambient conditions of the real world. Advances in probing techniques, such as 3D AFM, which enables imaging with an atomic resolution at liquid/solid interfaces,^[60,67] would move a step forward toward exploration and clarification of more realistic conditions. Overall, it still has a long way to go concerning how to bridge the pressure and material gap to extend the atomic-scale understanding and knowledge to enlighten ubiquitous hydration processes and corresponding applications behind chemistry, physics, and biology.

ACKNOWLEDGMENTS

The authors acknowledge financial support from the National Natural Science Foundation of China (Grants Nos. 22125203, 21790351), and the Fundamental Research Funds for the Central Universities (Grant No. 22120210365).

CONFLICT OF INTEREST

The authors declare that they have no conflict of interest.

ETHICS STATEMENT

The authors declare that they have no conflict of interest. No animal and human research studies were conducted in this paper.

DATA AVAILABILITY STATEMENT

The data that support the findings of this study are available from the corresponding author upon reasonable request.

ORCID

Wei Xu  <https://orcid.org/0000-0003-0216-794X>

REFERENCES

- W. Saenger, *Principles of Nucleic Acid Structure*, Springer-Verlag, New York, 1984.
- M. Hanus, F. Ryjáček, M. Kabeláč, T. Kubař, T. V. Bogdan, S. A. Trygubenko, P. Hobza, *J. Am. Chem. Soc.* **2003**, *125*, 7678.
- L. Gorb, J. Leszczynski, *J. Am. Chem. Soc.* **1998**, *120*, 5024.
- J. Gu, J. Leszczynski, *J. Phys. Chem. A* **1999**, *103*, 2744.
- J. Carrasco, A. Hodgson, A. Michaelides, *Nat. Mater.* **2012**, *11*, 667.
- J. Schiebel, R. Gaspari, T. Wulsdorf, K. Ngo, C. Sohn, T. E. Schrader, A. Cavalli, A. Ostermann, A. Heine, G. Klebe, *Nat. Commun.* **2018**, *9*, 3559.
- N. Nandi, K. Bhattacharyya, B. Bagchi, *Chem. Rev.* **2000**, *100*, 2013.
- A. W. Omta, M. F. Kropman, S. Woutersen, H. J. Bakker, *Science* **2003**, *301*, 347.
- I. A. Heisler, S. R. Meech, *Science* **2010**, *327*, 857.
- K. J. Tielrooij, N. Garcia-Araez, M. Bonn, H. J. Bakker, *Science* **2010**, *328*, 1006.
- J. Zhang, P. Chen, B. Yuan, W. Ji, Z. Cheng, X. Qiu, *Science* **2013**, *342*, 611.
- K. Kaiser, L. M. Scriven, F. Schulz, P. Gawel, L. Gross, H. L. Anderson, *Science* **2019**, *365*, 1299.
- D. J. Rizzo, G. Veber, T. Cao, C. Bronner, T. Chen, F. Zhao, H. Rodriguez, S. G. Louie, M. F. Crommie, F. R. Fischer, *Nature* **2018**, *560*, 204.
- D. J. Rizzo, G. Veber, J. Jiang, R. McCurdy, T. Cao, C. Bronner, T. Chen, S. G. Louie, F. R. Fischer, M. F. Crommie, *Science* **2020**, *369*, 1597.
- B. Cirera, A. Sánchez-Grande, B. de la Torre, J. Santos, S. Edalatmanesh, E. Rodríguez-Sánchez, K. Lauwaet, B. Mallada, R. Zbořil, R. Miranda, O. Gröning, P. Jelínek, N. Martín, D. Ecija, *Nat. Nanotechnol.* **2020**, *15*, 437.
- Q. Fan, L. Yan, M. W. Tripp, O. Krejčí, S. Dimosthenous, S. R. Kachel, M. Chen, A. S. Foster, U. Koert, P. Liljeroth, J. M. Gottfried, *Science* **2021**, *372*, 852.
- S. Mishra, G. Catarina, F. Wu, R. Ortiz, D. Jacob, K. Eimre, J. Ma, C. A. Pignedoli, X. Feng, P. Ruffieux, J. Fernández-Rossier, R. Fasel, *Nature* **2021**, *598*, 287.
- A. Verdager, G. M. Sacha, H. Bluhm, M. Salmeron, *Chem. Rev.* **2006**, *106*, 1478.
- M. L. Liriano, C. Gattinoni, E. A. Lewis, C. J. Murphy, E. C. H. Sykes, A. Michaelides, *J. Am. Chem. Soc.* **2017**, *139*, 6403.
- T. Mitsui, M. K. Rose, E. Fomin, D. F. Ogletree, M. Salmeron, *Science* **2002**, *297*, 1850.
- R. Schaub, P. Thostrup, N. Lopez, E. Lægsgaard, I. Stensgaard, J. K. Nørskov, F. Besenbacher, *Phys. Rev. Lett.* **2001**, *87*, 266104.
- L. R. Merte, G. Peng, R. Bechstein, F. Rieboldt, C. A. Farberow, L. C. Grabow, W. Kudernatsch, S. Wendt, E. Lægsgaard, M. Mavrikakis, F. Besenbacher, *Science* **2012**, *336*, 889.
- Y. He, A. Tilocca, O. Dulub, A. Selloni, U. Diebold, *Nat. Mater.* **2009**, *8*, 585.
- J. Cerdá, A. Michaelides, M. L. Bocquet, P. J. Feibelman, T. Mitsui, M. Rose, E. Fomin, M. Salmeron, *Phys. Rev. Lett.* **2004**, *93*, 116101.
- S. Maier, B. A. J. Lechner, G. A. Somorjai, M. Salmeron, *J. Am. Chem. Soc.* **2016**, *138*, 3145.
- S. Nie, P. J. Feibelman, N. C. Bartelt, K. Thürmer, *Phys. Rev. Lett.* **2010**, *105*, 026102.
- A. Michaelides, K. Morgenstern, *Nat. Mater.* **2007**, *6*, 597.
- J. Carrasco, A. Michaelides, M. Forster, S. Haq, R. Raval, A. Hodgson, *Nat. Mater.* **2009**, *8*, 427.
- H. Gawronski, J. Carrasco, A. Michaelides, K. Morgenstern, *Phys. Rev. Lett.* **2008**, *101*, 136102.
- T. Yamada, S. Tamamori, H. Okuyama, T. Aruga, *Phys. Rev. Lett.* **2006**, *96*, 036105.
- T. Kumagai, M. Kaizu, S. Hatta, H. Okuyama, T. Aruga, I. Hamada, Y. Morikawa, *Phys. Rev. Lett.* **2008**, *100*, 166101.
- A. Shiotari, Y. Sugimoto, *Nat. Commun.* **2017**, *8*, 14313.
- D. Stacchiola, J. B. Park, P. Liu, S. Ma, F. Yang, D. E. Starr, E. Muller, P. Sutter, J. Hrbek, *J. Phys. Chem. C* **2009**, *113*, 15102.
- J. Guo, X. Meng, J. Chen, J. Peng, J. Sheng, X. Z. Li, L. Xu, J. R. Shi, E. Wang, Y. Jiang, *Nat. Mater.* **2014**, *13*, 184.
- X. Meng, J. Guo, J. Peng, J. Chen, Z. Wang, J.-R. Shi, X.-Z. Li, E.-G. Wang, Y. Jiang, *Nat. Phys.* **2015**, *11*, 235.
- J. Chen, J. Guo, X. Meng, J. Peng, J. Sheng, L. Xu, Y. Jiang, X. Z. Li, E. G. Wang, *Nat. Commun.* **2014**, *5*, 4056.
- J. Henzl, K. Boom, K. Morgenstern, *J. Am. Chem. Soc.* **2014**, *136*, 13341.
- K. Lucht, D. Loose, M. Ruschmeier, V. Strötkotter, G. Dyker, K. Morgenstern, *Angew. Chem. Int. Ed.* **2018**, *57*, 1266.
- K. Lucht, K. Morgenstern, *J. Chem. Phys.* **2021**, *154*, 014701.
- J. Henzl, K. Boom, K. Morgenstern, *J. Chem. Phys.* **2015**, *142*, 101920.
- K. Lucht, I. Trosien, W. Sander, K. Morgenstern, *Angew. Chem. Int. Ed.* **2018**, *57*, 16334.
- C. Lin, G. R. Darling, M. Forster, F. McBride, A. Massey, A. Hodgson, *J. Am. Chem. Soc.* **2020**, *142*, 13814.
- S. A. Trygubenko, T. V. Bogdan, M. Rueda, M. Orozco, F. J. Luque, J. Sponer, P. Slavíček, P. Hobza, *Phys. Chem. Chem. Phys.* **2002**, *4*, 4192.
- M. Hanus, M. Kabeláč, J. Rejnek, F. Ryjáček, P. Hobza, *J. Phys. Chem. B* **2004**, *108*, 2087.
- J. Rejnek, M. Hanus, M. Kabeláč, F. Ryjáček, P. Hobza, *Phys. Chem. Chem. Phys.* **2005**, *7*, 2006.
- H. Langer, N. L. Doltsinis, *J. Chem. Phys.* **2003**, *118*, 5400.
- R. X. He, X. H. Duan, X. Y. Li, *Phys. Chem. Chem. Phys.* **2006**, *8*, 587.
- C. Zhang, L. Xie, Y. Ding, Q. Sun, W. Xu, *ACS Nano* **2016**, *10*, 3776.
- H. Kong, Q. Sun, L. Wang, Q. Tan, C. Zhang, K. Sheng, W. Xu, *ACS Nano* **2014**, *8*, 1804.
- C. Zhang, L. Wang, L. Xie, H. Kong, Q. Tan, L. Cai, Q. Sun, W. Xu, *ChemPhysChem* **2015**, *16*, 2099.
- C. Zhang, L. Xie, L. Wang, H. Kong, Q. Tan, W. Xu, *J. Am. Chem. Soc.* **2015**, *137*, 11795.
- D. Li, L. Sun, Y. Ding, M. Liu, L. Xie, Y. Liu, L. Shang, Y. Wu, H. J. Jiang, L. Chi, X. Qiu, W. Xu, *ACS Nano* **2021**, *15*, 16896.

53. C. Zhang, L. Xie, Y. Ding, W. Xu, *Chem. Commun.* **2018**, 54, 771.
54. L. Xie, H. Jiang, D. Li, M. Liu, Y. Ding, Y. Liu, X. Li, X. Li, H. Zhang, Z. Hou, Y. Luo, L. Chi, X. Qiu, W. Xu, *ACS Nano* **2020**, 14, 10680.
55. R. Otero, M. Lukas, R. E. Kelly, W. Xu, E. Lægsgaard, I. Stensgaard, L. N. Kantorovich, F. Besenbacher, *Science* **2008**, 319, 312.
56. R. E. Kelly, W. Xu, M. Lukas, R. Otero, M. Mura, Y. J. Lee, E. Lægsgaard, I. Stensgaard, L. N. Kantorovich, F. Besenbacher, *Small* **2008**, 4, 1494.
57. Y. Ding, X. Wang, D. Li, L. Xie, W. Xu, *ACS Nano* **2019**, 13, 6025.
58. Y. Ding, L. Xie, X. Yao, C. Zhang, W. Xu, *Fundamental Research* **2021**, <https://doi.org/10.1016/j.fmre.2021.10.005>.
59. J. Peng, D. Cao, Z. He, J. Guo, P. Hapala, R. Ma, B. Cheng, J. Chen, W. J. Xie, X. Z. Li, P. Jelínek, L. M. Xu, Y. Q. Gao, E. G. Wang, Y. Jiang, *Nature* **2018**, 557, 701.
60. J. Peng, J. Guo, R. Ma, Y. Jiang, *Surf. Sci. Rep.* 100549, **2021**, <https://doi.org/10.1016/j.surfrep.2021.100549>.
61. J. Peng, J. Guo, R. Ma, X. Meng, Y. Jiang, *J. Phys.: Condens. Matter* **2017**, 29, 104001.
62. S. Song, N. Guo, X. Li, G. Li, Y. Haketa, M. Telychko, J. Su, P. Lyu, Z. Qiu, H. Fang, X. Peng, J. Li, X. Wu, Y. Li, C. Su, M. J. Koh, J. Wu, H. Maeda, C. Zhang, J. Lu, *J. Am. Chem. Soc.* **2020**, 142, 13550.
63. R. Ma, D. Cao, C. Zhu, Y. Tian, J. Peng, J. Guo, J. Chen, X. Z. Li, J. S. Francisco, X. C. Zeng, L. M. Xu, E. G. Wang, Y. Jiang, *Nature*, **2020**, 577, 60.
64. J. Peng, J. Guo, P. Hapala, D. Cao, R. Ma, B. Cheng, L. Xu, M. Ondráček, P. Jelínek, E. Wang, Y. Jiang, *Nat. Commun.* **2018**, 9, 122.
65. J. Xu, X. Zhu, S. Tan, Y. Zhang, B. Li, Y. Tian, H. Shan, X. Cui, A. Zhao, Z. Dong, J. Yang, Y. Luo, B. Wang, J. G. Hou, *Science* **2021**, 371, 818.
66. C. Zhang, R. B. Jaculbia, Y. Tanaka, E. Kazuma, H. Imada, N. Hayazawa, A. Muranaka, M. Uchiyama, Y. Kim, *J. Am. Chem. Soc.* **2021**, 143, 9461.
67. T. Fukuma, Y. Ueda, S. Yoshioka, H. Asakawa, *Phys. Rev. Lett.* **2010**, 104, 016101.

AUTHOR BIOGRAPHIES



Chi Zhang received her bachelor and PhD degrees in engineering from Tongji University (School of Materials Science and Engineering), China in 2012 and 2017 under the supervision of Prof. Wei Xu. Thereafter, she was engaged in the postdoctoral research in RIKEN, Japan from 2018 to 2021 (supervisor: Dr. Yousoo Kim, chief scientist). Since 2021, she started working in the School of Materials Science and Engineering at Tongji University,

China as a professor. Her main research interests are on-surface molecular self-assembly and on-surface chemical reactions aiming at fundamental understandings of interfacial chemical processes.



Wei Xu received his PhD degree in science from Aarhus University, Denmark in 2008. Thereafter he was a postdoctoral fellow at Interdisciplinary Nanoscience Center (iNANO), Aarhus University, Denmark and at Departments of Chemistry and Physics, The Penn State University, USA. Since 2009, he has been a full professor at Tongji University, P.R. China. His main research interests are Scanning Tunneling Microscopy (STM) and Density Functional Theory (DFT) investigations of molecular self-assemblies and reactions on surfaces under ultrahigh vacuum conditions with the aim of controllably building functional surface nanostructures and gaining fundamental insights into physics and chemistry.

How to cite this article: C. Zhang, W. Xu, *Aggregate* **2022**, e175. <https://doi.org/10.1002/agt2.175>